

The Open Nucleotide Pocket of the Profilin/Actin X-Ray Structure Is Unstable and Closes in the Absence of Profilin

T. J. Minehardt,* P. A. Kollman,* R. Cooke,^{†‡} and E. Pate[§]

*Department of Pharmaceutical Chemistry and [†]Department of Biochemistry and Biophysics, and [‡]Cardiovascular Research Institute, University of California, San Francisco, California; and [§]Department of Mathematics, Washington State University, Pullman, Washington

ABSTRACT The open nucleotide pocket conformation of actin in the profilin:actin•CaATP x-ray structure has been hypothesized to be a crucial intermediate for nucleotide exchange in the actin depolymerization/polymerization cycle. The requirement for ancillary modification of actin for crystallization leads to ambiguities in this interpretation, however. We have used molecular dynamics simulations to model the thermodynamic properties of the actin x-ray structure, outside the crystal lattice, in an aqueous environment with profilin removed. Our simulations show that the open-nucleotide-pocket, profilin-free structure is actually unstable, and closes. The coordination of actin to the nucleotide in the molecular-dynamics-derived closed structure is virtually identical to that in the closed profilin:actin•SrATP x-ray structure. Thus, there is currently no thermodynamically stable structure representing the open-nucleotide-pocket state of actin.

INTRODUCTION

The cycling of actin between the monomeric G-actin species and filamentous F-actin is a dynamic process, with the equilibrium between the two species dependent upon immediate cellular needs. The transition serves as an integral part of the function of eukaryotic cells, with polymerized F-actin both providing a structural role in cells and functioning as an obligatory component of myosin-based motility (1). The initial x-ray structure of G-actin showed it to be a globular protein comprised of four contiguous subdomains (Fig. 1) (2). There is a nucleotide-binding site between the lobes of the protein formed by subdomains 1 and 2, and by subdomains 3 and 4, with the nucleotide interacting with all four subdomains. Although modulated by actin-associated proteins, ATP at the nucleotide site of G-actin favors polymerization at the barbed-end of the actin filament, whereas the posthydrolysis, ADP-bound state favors depolymerization at the pointed end (reviewed in Pollard et al. (3) and references therein). The requirement for nucleotide exchange in a polymerization-depolymerization cycle has been taken to imply that an opening and closing of the nucleotide-binding site is associated with movements of the subdomains, and that these nucleotide-dependent domain movements are involved in the G-/F-actin transition. Thus, there has been intense interest in attempting to understand the relationship between subdomain movements in actin, the opening and closing of the nucleotide site, and the bound nucleotide.

The most compelling, and frequently quoted, structural evidence for an open conformation of the actin nucleotide site has come from the x-ray crystallography structure of the open nucleotide binding site structure of the profilin:actin•CaATP complex. This open nucleotide site conformation (Protein Data Bank 1HLU (4)), coupled with previous observations that profilin promotes nucleotide exchange (5–8), has led to wide postulation that this structure is the open structure of actin for nucleotide exchange (reviewed in Schuler (9) and Sablin et al. (10), and references therein). Others have challenged this assignment (11,12).

Difficulties arise with interpretation. This is due to the fact that x-ray structures of actin have only been possible when the polymerization of G-actin has been inhibited either by complexing G-actin with ancillary proteins such as DNAase, profilin, gelsolin, vitamin D-binding protein, etc. (2,4,13–16), by complexing it with drugs (17), or via covalent modification of actin by the binding of organic molecules (11,12). Ambiguities thus arise as to whether the properties of the x-ray structures of the modified proteins represent true properties of actin or are simply the result of the modifications necessary for crystallization. All current actin x-ray structures have a closed nucleotide-binding site, with the single exception of the profilin:actin•CaATP structure (4) discussed above.

Molecular dynamics (MD) simulations can provide a valuable tool for helping to sort out the ambiguities present in the x-ray database associated with protein modification. For MD simulation, the ancillary bound proteins or covalent modifications can be easily removed. The thermodynamic properties of the remaining native protein in the absence of crystal packing forces can then be examined in a modeled aqueous environment under physiological conditions. Of equal importance, parallel MD simulations with retention of the ancillary protein modification can further provide control

Submitted August 22, 2005, and accepted for publication December 28, 2005.

This article is dedicated to deceased colleague P. A. Kollman.

Address reprint requests to E. Pate, Dept. of Mathematics, Washington State University, Pullman, WA 99164. Tel.: 509-335-3151; Fax: 509-335-1188; E-mail: epate@wsu.edu.

T. J. Minehardt's present address is Lone Star Biotechnologies, Austin, TX 78736.

© 2006 by the Biophysical Society

0006-3495/06/04/2445/05 \$2.00

doi: 10.1529/biophysj.105.072900

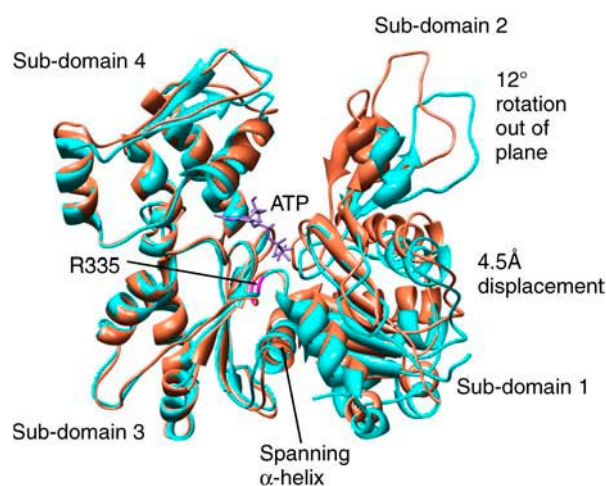


FIGURE 1 Open-nucleotide-pocket x-ray structure of actin•CaATP without profilin (cyan, Protein Data Bank 1HLU) and the structure after 1000 ps of MD simulation (tan) are shown. Structures have been superimposed via a least-squares distance minimization ($C\alpha$ coordinates) of subdomains 3 and 4. The four subdomains of actin are labeled. ATP is shown in purple. The nucleotide-binding site has closed in the tan structure due to a 4.5-Å displacement of subdomain 1 (a significant component is out of the plane of the page) and a 12° rotation of subdomain 2, both movements relative to subdomains 3 and 4. The $C\alpha$ - $C\alpha$ distance across the ATP triphosphate-binding domain decreases by 2.6 Å. R335 is shown in magenta. A Protein Data Bank format file (Word) of the structure of actin•CaATP with profilin removed after 1000 ps of MD simulation is available at http://www.math.wsu.edu/faculty/pate/actin_1000ps.doc.

comparisons with the x-ray crystallography results. We use this approach to demonstrate that the open nucleotide-site actin structure is unstable in the absence of profilin, and closes to a structure with a nucleotide site resembling that in the closed profilin:actin•SrATP x-ray structure (13).

METHODS

Molecular dynamics simulations were performed using the Amber 7 (18) suite of codes and the Cornell force field (19). The structures of profilin:actin•CaATP (Protein Data Bank 1HLU, ref. (4)) and profilin:actin•SrATP (Protein Data Bank 2BTF (13)) were used as the starting points for simulation. For simulations in the absence of profilin, the coordinates of profilin were manually edited out of the PDB file. For simulations of nucleotide-free actin states, ATP and the metal ion were also edited out of the file. To substitute between SrATP and CaATP at the active site, ATP was retained in the PDB file and the metal ion alone was changed. ADP was simulated at the nucleotide site by deleting the γ -phosphate moiety from ATP in the PDB file. Charges for ATP and ADP were determined by first performing a single-point energy calculation at the Hartree-Fock level of theory using a 6-31G* basis set to obtain electrostatic charges. These are then fit to the molecules using the restrained electrostatic potential procedure (20). Van der Waals parameters for Ca^{2+} and Sr^{2+} were taken from Aqvist (21). The tLeap module of Amber 7 was used to add hydrogens to the x-ray structures for simulation. Histidines were protonated as appropriate for their local environment. Na^+ counterions were then added to produce overall charge neutrality. A box of TIP3P water molecules (22) was used to solvate the system, with a 10-Å border between the edge of the box and the closest point on the protein surface. The total size of all simulations was >78,000 atoms.

The entire protein-water system was energy-minimized using 500 steps of the steepest descent algorithm and a subsequent 500 steps of the conjugate gradient algorithm. The minimized system was then gradually heated and maintained at 300 K using the Berendsen algorithm (23) for maintenance of temperature via coupling to an external bath. The particle-mesh Ewald procedure (24–26) with a nonbonded cutoff of 8 Å was used to handle electrostatic interactions. MD simulations employed the SHAKE algorithm (27) and a 2-fs time step. More limited simulations employing a 0.1-fs time step yielded similar results. Unless otherwise stated, all simulations were for 1000 ps. Periodic boundary conditions were employed at constant pressure. Simulation results were visualized using the Midas (28) and Chimera (29) molecular graphics suites of codes.

RESULTS

We performed MD simulations based upon the open nucleotide site profilin:actin•CaATP x-ray structure (4) to investigate the implications of protein modification. The results of these simulations were compared with simulation of the corresponding profilin:actin•SrATP structure (13) from the same laboratory, but containing a closed nucleotide-binding site. Two simulations were initially done. In the first, the profilin:actin•CaATP structure with an open nucleotide-binding site was taken directly from the Protein Data Bank and simulated in a full box of explicit waters. The MD simulation showed virtually no change in the structure. The open nucleotide-binding site remained open. The root mean-square (RMS) displacement ($C\alpha$ atoms) between the profilin:actin•CaATP x-ray structure and the stable structure obtained after 1000 ps of MD simulation was <0.2 Å. Thus, the MD simulation and x-ray crystallography agree that the open-nucleotide-site, profilin:actin•CaATP x-ray structure is stable under modeled physiological conditions. For the second simulation, profilin was now deleted from the x-ray structure of the profilin:actin•CaATP complex. The open nucleotide site of the remaining, isolated G-actin x-ray structure now rapidly closed down during the MD simulation. Profilin binds across both subdomains 1 and 3 of actin (4,13), making it structurally plausible that profilin could be stabilizing an otherwise globally strained conformation (see Fig. 1). Indeed, the major portion of the conformational change observed occurred within the first 200 ps of the MD simulation, demonstrating that the profilin-free actin complex was indeed quite unstable. The RMS displacement of the MD-simulated structure as a function of time from the initial x-ray structure is shown in Fig. 2.

More important, the open nucleotide site evolved into a closed structure topologically similar to that previously described in the related x-ray structure of the profilin:actin•SrATP complex from the same lab containing a closed nucleotide site (13). Comparison of the initial open actin structure and the MD-simulated closed actin structure obtained after 1000 ps of simulation showed a clamshell closing of the nucleotide site resulting from movements of subdomains 1 and 2 relative to subdomains 3 and 4 (Fig. 1). The transition from the open to the closed conformation could be modeled by

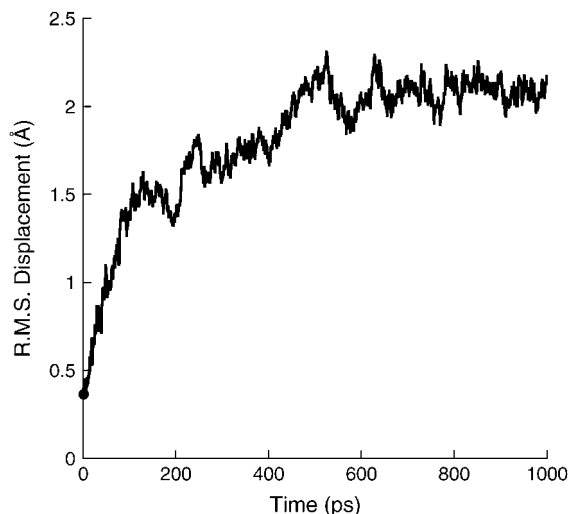


FIGURE 2 Root mean-square displacement of the MD-simulated actin•ATP structure in the absence of profilin as a function of time. The nonzero intercept (●) represents the displacement that occurred during the energy minimization process after removal of profilin. A new equilibrium is reached after ~ 500 ps.

changes in backbone ϕ -angles of -5° at R335 and of -10° , 12° , -16° , and -13° at A138, G146, R147, and T149, respectively, in the open-nucleotide-site structure. The important point in comparing the MD simulation results with previous crystallographic analysis is that R335 and the spanning α -helix and adjacent loop between subdomains 1 and 3 containing amino acids 138–149 (Fig. 1) are the identical structural elements that have previously been identified as being involved in the closing of the nucleotide pocket in the actin x-ray structures (4,11,13,30). Further evidence for changes in the vicinity of R335 and the spanning α -helix comes from the observations that the average magnitudes of the differences between ϕ/ψ -angles (average $\Delta\phi$ and $\Delta\psi$) in the open x-ray structure and the MD-simulated structure in the region P333–Y337 are $21.7^\circ/25.2^\circ$ and $11.8^\circ/11.4^\circ$ for the region A138–T149. The MD simulation thus reproduces previous crystallographic observations. The net effect is a rotation and translation of subdomains 1 and 2 relative to subdomains 3 and 4, as shown in Fig. 1. An examination of the RMS displacement of the MD-simulated, closed-nucleotide-site actin structure as a function of time demonstrated that a new equilibrium had been reached at 1000 ps (Fig. 2).

The MD simulation with profilin removed yields a 2.6-Å closing of the triphosphate-binding pocket (distance measured as S14 \leftrightarrow G158, C α \leftrightarrow C α). This is virtually identical to the 2.7-Å closing observed between the open and closed x-ray structures of the profilin:actin•ATP x-ray complexes (4,13). Fig. 3 shows in greater detail the correspondence between the nucleotide-binding domains. As is evident in Fig. 3, the hydrogen bonding patterns are virtually identical. Hydrogen atoms cannot be resolved in x-ray structures, but are present in the MD simulation, which must be taken into

consideration when comparing hydrogen bond lengths. The only difference between the interactions of protein with the nucleotide is that a water molecule is trapped in the closing of the nucleotide-binding site in the MD simulation, mediating hydrogen-bonding interactions between the backbone amide groups of G15 and M16 with the β -phosphate of ATP. These are instead direct hydrogen bonds in the closed profilin: actin•SrATP x-ray structure (red hydrogen bonding patterns, Fig. 3). The water appeared at the nucleotide site during the initial solvation of the x-ray structure in a box of explicit water molecules, and remained stable for the duration of the simulation. After MD simulation, H73 also now forms a hydrogen bond across the cleft to the backbone oxygen of G158 as seen in the closed x-ray structure. The hydrophobic interaction of the adenine ring with the ethyl groups on the side chain of E214 is also preserved (detail not shown in Fig. 3). The crucial point that must be considered in the evaluation of the results of an MD simulation is the degree to which the atomic-level force field employed in the simulation accurately captures the true forces involved. The existing x-ray structure of the closed-pocket, actin•nucleotide structure (13) serves as the gold standard for this comparison. As shown above, our results indicate excellent agreement between the closed structure to which the MD simulation evolves and an actual x-ray structure.

An additional advantage of MD simulation is that we could perform the following control simulations to provide additional confidence in the conclusions. 1), MD simulations of the closed nucleotide site profilin:actin•SrATP structure remained closed whether profilin was present or absent. 2), MD simulations of the structure resulting from the substitution of SrATP for CaATP, or with the elimination of CaATP (apo structure) in the profilin:actin•CaATP x-ray structure, while retaining profilin, remained open. 3), MD simulation of the structure resulting from the substitution of SrATP for CaATP in the actin•CaATP structure (profilin removed for the simulation) showed a closing of the nucleotide site. 4), MD simulation of the profilin:actin•CaATP structure with profilin removed and CaATP replaced with CaADP showed a closing of the nucleotide site. 5), MD simulation of the profilin:actin•CaATP structure with both profilin and CaATP removed (open apo structure) continued to show a closing of the nucleotide site. This latter simulation implied that the domain movements we were seeing were the result of instabilities generated in the fundamental protein structure resulting from the interaction with profilin, and not simply the result of charge effects at the nucleotide site. In summary, all combinations of closed x-ray structures examined remained closed during MD simulation. All combinations of open profilin: actin•nucleotide complexes remained open. In the absence of profilin, all open actin structures closed down. These control simulations provide further confidence in the generality of our conclusions. The open structure in the absence of profilin evolves into a structure homologous to other closed actin structures. We also note that in all simulations, with and

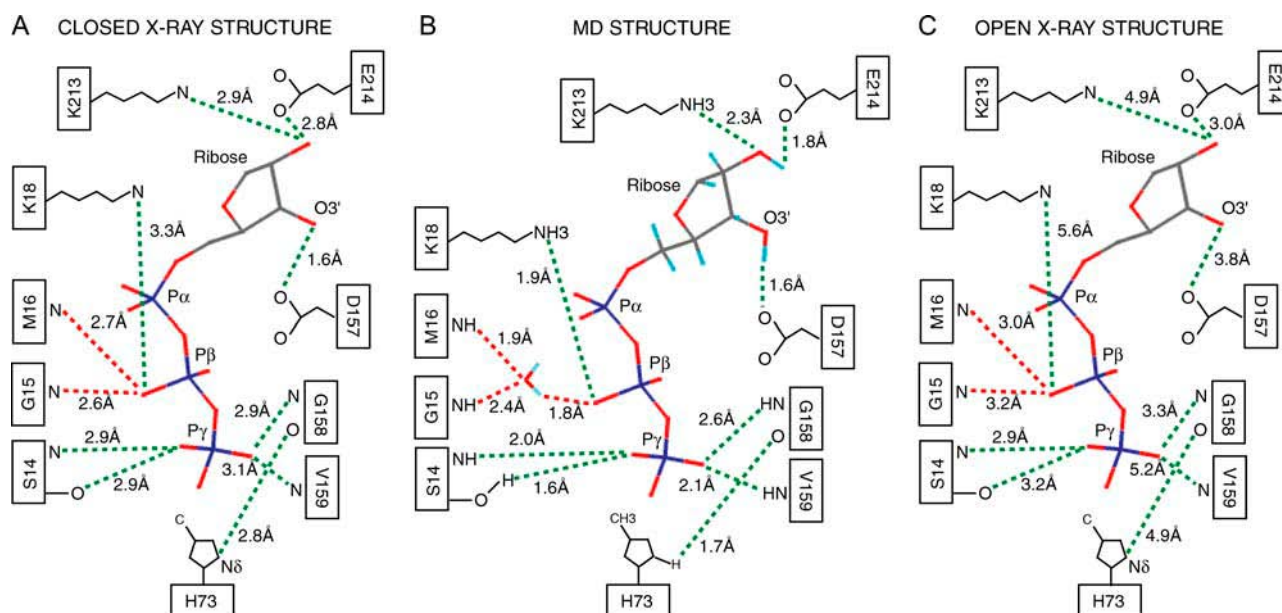


FIGURE 3 (A) Hydrogen-bonding pattern of the closed nucleotide site of profilin:actin•SrATP x-ray structure is shown. (B) The hydrogen-bonding pattern after 1000 ps MD simulation of the profilin:actin•CaATP x-ray structure with profilin removed is shown after the nucleotide site had closed. Adenine is omitted from the structures of ATP to enhance detail. (C) Distances in the open profilin:actin•CaATP x-ray structure are shown for comparison. Hydrogen atoms are not resolved in the x-ray structures. They are present in the MD simulation. In A and B, the two hydrogen-bonding patterns are virtually identical. The only difference is that a water molecule is trapped during the closing of the nucleotide pocket in the MD simulation (*right*) and now mediates the hydrogen bonding to the β -phosphate moiety of ATP. Green dashed lines show hydrogen bonds conserved between the two closed structures (A and B). Red dashed lines show the water-mediated hydrogen bond. Color scheme: cyan, hydrogen; gray, carbon; red, oxygen; and blue, phosphorus.

without profilin, the DNAase binding loop (D-loop) remained a loop.

DISCUSSION

The dynamic polymerization/depolymerization cycle of actin requires nucleotide hydrolysis and exchange of ADP for ATP. Thus, considerable effort has been directed at identifying nucleotide-site conformational changes and their relationship to the global conformational changes associated with polymerization. Studies using proteolysis, fluorescence, and binding as the reporter signal (31–38) have all been consistent with the presence of nucleotide-site conformational changes in actin. Recent control experimental investigations taking advantage of a known x-ray actin structure, however, have suggested that these localized reporter signals may not always signal a nucleotide cleft opening (39). Electron microscopy reconstructions of actin filaments have implied that the actin cleft is more open in the ADP-bound state compared to the ATP-bound state (10,40). However, these EM studies were done with yeast actin, which may show significant differences from vertebrate skeletal muscle actin. The presence of open nucleotide sites in the x-ray structures of proteins such as nucleotide-free and glucose-free hexokinase (41), nucleotide-free Arp2, Arp3 (42), and ParM (43), all of which share the homologous “actin fold” (44), has further argued for an open state in actin (11). It is important

to emphasize that our results do not preclude an open state in actin. However, they do indicate that a stable atomic level structure is not in hand, and conclusions based on the present open structure must be evaluated with this in mind.

In summary, our results support previous suggestions that profilin facilitates nucleotide exchange in actin (5–8). However, the MD simulations imply that profilin does so by stabilizing an otherwise thermodynamically unstable, open-nucleotide-pocket state of actin. The MD simulations imply that the open-nucleotide-site actin structure state is not on the *in vivo* nucleotide-exchange pathway.

This work was supported by National Institutes of Health grants AR39643 (to E.P.), AR42895 (to R.C.), GM29072 (to P.A.K.). Computer simulations were also supported by a grant from the National Science Foundation (MCB040031N), and utilized the Xeon Cluster at the National Center for Supercomputer Applications. Molecular visualizations were done using the University of California at San Francisco Computer Graphics Laboratory, supported by a National Institutes of Health grant RR001081 to T. Ferrin.

REFERENCES

1. Alberts, B., K. Roberts, J. Lewis, M. Raff, P. Walter, and A. Johnson. 2002. *Molecular Biology of the Cell*, 4th ed. Garland, New York.
2. Kabsch, W., H. G. Mannherz, D. Suck, E. F. Pai, and K. C. Holmes. 1990. Atomic structure of the actin:DNase I complex. *Nature*. 347: 37–44.
3. Pollard, T. D., L. Blanchoin, and R. D. Mullins. 2000. Molecular mechanisms controlling actin filament dynamics in nonmuscle cells. *Annu. Rev. Biophys. Biomol. Struct.* 29:545–576.

4. Chik, J. K., U. Lindberg, and C. E. Schutt. 1996. The structure of an open state of beta-actin at 2.65 Å resolution. *J. Mol. Biol.* 263:607–623.
5. Mockrin, S. C., and E. D. Korn. 1980. *Acanthamoeba* profilin interacts with G-actin to increase the rate of exchange of actin-bound adenosine 5'-triphosphate. *Biochemistry*. 19:5359–5362.
6. Nishida, E. 1985. Opposite effects of cofilin and profilin from porcine brain on rate of exchange of actin-bound adenosine 5'-triphosphate. *Biochemistry*. 24:1160–1164.
7. Goldschmidt-Clermont, P. J., L. M. Machesky, S. K. Doberstein, and T. D. Pollard. 1991. Mechanism of the interaction of human platelet profilin with actin. *J. Cell Biol.* 113:1081–1089.
8. Vinson, V. K., E. M. De La Cruz, H. N. Higgs, and T. D. Pollard. 1998. Interactions of *Acanthamoeba* profilin with actin and nucleotides bound to actin. *Biochemistry*. 37:10871–10880.
9. Schuler, H. 2001. ATPase activity and conformational changes in the regulation of actin. *Biochim. Biophys. Acta.* 1549:137–147.
10. Sablin, E. P., J. F. Dawson, M. S. VanLoock, J. A. Spudich, E. H. Egelman, and R. J. Fletterick. 2002. How does ATP hydrolysis control actin's associations? *Proc. Natl. Acad. Sci. USA.* 99:10945–10947.
11. Graceffa, P., and R. Dominguez. 2003. Crystal structure of monomeric actin in the ATP state. Structural basis of nucleotide-dependent actin dynamics. *J. Biol. Chem.* 278:34172–34180.
12. Otterbein, L. R., P. Graceffa, and R. Dominguez. 2001. The crystal structure of uncomplexed actin in the ADP state. *Science*. 293:708–711.
13. Schutt, C. E., J. C. Myslik, M. D. Rozycki, N. C. Goonesekere, and U. Lindberg. 1993. The structure of crystalline profilin-beta-actin. *Nature*. 365:810–816.
14. Dawson, J. F., E. P. Sablin, J. A. Spudich, and R. J. Fletterick. 2003. Structure of an F-actin trimer disrupted by gelsolin and implications for the mechanism of severing. *J. Biol. Chem.* 278:1229–1238.
15. Otterbein, L. R., C. Cosio, P. Graceffa, and R. Dominguez. 2002. Crystal structures of the vitamin D-binding protein and its complex with actin: structural basis of the actin-scavenger system. *Proc. Natl. Acad. Sci. USA.* 99:8003–8008.
16. Vorobiev, S., B. Strokopytov, D. G. Drubin, C. Frieden, S. Ono, J. Condeelis, P. A. Rubenstein, and S. C. Almo. 2003. The structure of nonvertebrate actin: implications for the ATP hydrolytic mechanism. *Proc. Natl. Acad. Sci. USA.* 100:5760–5765.
17. Klenchin, V. A., J. S. Allingham, R. King, J. Tanaka, G. Marriott, and I. Rayment. 2003. Trisoxazole macrolide toxins mimic the binding of actin-capping proteins to actin. *Nat. Struct. Biol.* 10:1058–1063.
18. Case, D. A., D. A. Perlman, J. W. Caldwell, T. E. Cheatham III, J. Wang, W. S. Ross, C. L. Simmerling, T. A. Darden, K. M. Merz, R. V. Stanton, A. L. Cheng, J. J. Vincent, M. Crowley, V. Tsui, H. Gohlke, R. J. Radmer, Y. Duan, J. Pitera, I. Massova, G. L. Seibel, U. K. Singh, P. K. Weiner, and P. A. Kollman. 2002. *AMBER*. University of California, San Francisco.
19. Cornell, W. D., P. Cieplak, C. I. Bayly, I. R. Gould, K. M. Merz, D. M. Ferguson, D. C. Spellmeyer, T. Fox, J. W. Caldwell, and P. A. Kollman. 1995. A second generation force field for the simulation of proteins. *J. Am. Chem. Soc.* 117:5179–5197.
20. Bayly, C. I., W. D. Cieplak, W. D. Cornell, and P. A. Kollman. 1993. A well-behaved electrostatic potential based method using charge restraints for deriving atomic charges: the RESP model. *J. Phys. Chem.* 97:10269–10280.
21. Aqvist, J. 1992. Modelling of ion-ligand interactions in solutions and biomolecules. *J. Mol. Struct. (Theochem.)* 256:135–152.
22. Jorgensen, W. L., J. Chandrasekar, J. D. Madura, R. W. Impey, and M. L. Klein. 1983. Comparison of simple potential functions for simulating liquid water. *J. Comput. Phys.* 79:926–935.
23. Berendsen, H. J. C., J. P. M. Postma, W. F. v. Gunsteren, A. DiNola, and J. R. Ghaak. 1984. Molecular dynamics with coupling to an external bath. *J. Chem. Phys.* 113:3684–3690.
24. Darden, T., and D. York. 1993. Particle mesh Ewald: an Nlog(N) method for Ewald sums in large systems. *J. Chem. Phys.* 98:10089–10092.
25. Essman, U., M. Preera, T. Berkowitz, H. Darden, and G. Pedersen. 1995. A smooth particle mesh Ewald method. *J. Chem. Phys.* 103:8577–8593.
26. Hawkins, G. D., C. J. Cramer, and D. G. Truhlar. 1996. Parameterized models of aqueous free energies of solvation based on pairwise descreening of solute atomic charges from a dielectric medium. *J. Chem. Phys.* 100:19824–19839.
27. Ryckaert, A. J., G. Cicciotti, and H. J. C. Berendsen. 1977. Numerical integration of the cartesian equations of motion of a system with constraints: molecular dynamics of *n*-alkanes. *J. Comput. Phys.* 23:327–341.
28. Ferrin, T. E., C. C. Huang, L. E. Jarvis, and R. Langridge. 1988. The MIDAS display system. *J. Mol. Graph.* 6:13–27.
29. Pettersen, E. F., T. D. Goddard, C. C. Huang, G. S. Couch, D. M. Greenblatt, E. C. Meng, and T. E. Ferrin. 2004. UCSF Chimera—a visualization system for exploratory research and analysis. *J. Comput. Chem.* 25:1605–1612.
30. Page, R., U. Lindberg, and C. E. Schutt. 1998. Domain motions in actin. *J. Mol. Biol.* 280:463–474.
31. Strzelecka-Golaszewska, H. 2001. Divalent cations, nucleotides, and actin structure. *Results Probl. Cell Differ.* 32:23–41.
32. Strzelecka-Golaszewska, H., J. Moraczewska, S. Y. Khaitlina, and M. Mossakowska. 1993. Localization of the tightly bound divalent-cation-dependent and nucleotide-dependent conformation changes in G-actin using limited proteolytic digestion. *Eur. J. Biochem.* 211:731–742.
33. Schuler, H., C. E. Schutt, U. Lindberg, and R. Karlsson. 2000. Covalent binding of ATPgammaS to the nucleotide-binding site in S14C-actin. *FEBS Lett.* 476:155–159.
34. Kinoshita, H. J., L. A. Selden, J. E. Estes, and L. C. Gershman. 1993. Nucleotide binding to actin. Cation dependence of nucleotide dissociation and exchange rates. *J. Biol. Chem.* 268:8683–8691.
35. Muhrad, A., P. Cheung, B. C. Phan, C. Miller, and E. Reisler. 1994. Dynamic properties of actin. Structural changes induced by beryllium fluoride. *J. Biol. Chem.* 269:11852–11858.
36. Schuler, H., U. Lindberg, C. E. Schutt, and R. Karlsson. 2000. Thermal unfolding of G-actin monitored with the DNase I-inhibition assay stabilities of actin isoforms. *Eur. J. Biochem.* 267:476–486.
37. Mossakowska, M., J. Moraczewska, S. Khaitlina, and H. Strzelecka-Golaszewska. 1993. Proteolytic removal of three C-terminal residues of actin alters the monomer-monomer interactions. *Biochem. J.* 289:897–902.
38. Strzelecka-Golaszewska, H., A. Wozniak, T. Hult, and U. Lindberg. 1996. Effects of the type of divalent cation, Ca²⁺ or Mg²⁺, bound at the high-affinity site and of the ionic composition of the solution on the structure of F-actin. *Biochem. J.* 316:713–721.
39. Kudryashov, D. S., and E. Reisler. 2003. Solution properties of tetramethylrhodamine-modified G-actin. *Biophys. J.* 85:2466–2475.
40. Belmont, L. D., A. Orlova, D. G. Drubin, and E. H. Egelman. 1999. A change in actin conformation associated with filament instability after Pi release. *Proc. Natl. Acad. Sci. USA.* 96:29–34.
41. Anderson, C. M., R. E. Stenkamp, R. C. McDonald, and T. A. Steitz. 1978. A refined model of the sugar binding site of yeast hexokinase B. *J. Mol. Biol.* 123:207–219.
42. Robinson, R. C., K. Turbedsky, D. A. Kaiser, J. B. Marchand, H. N. Higgs, S. Choe, and T. D. Pollard. 2001. Crystal structure of Arp2/3 complex. *Science*. 294:1679–1684.
43. van den Ent, F., J. Moller-Jensen, L. A. Amos, K. Gerdes, and J. Lowe. 2002. F-actin-like filaments formed by plasmid segregation protein ParM. *EMBO J.* 21:6935–6943.
44. Kabsch, W., and K. C. Holmes. 1995. The actin fold. *FASEB J.* 9:167–174.